

# UNDERGRADUATE RESEARCH SYMPOSIUM

July • 24 • 2020 | 1:30 - 4:00 PM EST

Zoom: <https://zoom.us/j/93191593690> | Password: 358615

Welcome Address

1:30 PM EST

Rebecca Wells and Ram Dixit, Directors of Education



Image Analysis to Examine Spatial Properties of the Pericellular Matrix within 3D Hydrogels

1:35 PM

**Bruce Enzmann, Johns Hopkins University**  
**Burdick Lab (Penn)**



Patterning Hydrogel Thin Films for Inducing Cardiomyocyte Alignment

1:47 PM

**Joenid Colón-Mateo, UPR-Cayey**  
**Andrea Plaza-Castro, UPR-Cayey**  
**Christian Tessman, Johns Hopkins University**  
**Guvendiren Lab (NJIT)**



Viscoelastic Properties of Tofu as a Phantom for Liver Disease Diagnosis

2:00 PM

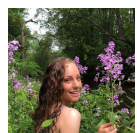
**Katherine Kerr, Purdue University**  
**Janmey Lab (Penn)**



Measuring and Modeling How Turgor Pressure-Driven Mechanical Forces Between Guard and Pavement Cells Underlie Stomatal Opening and Closing

2:12 PM

**Mythili Subbanna, Amherst College**  
**Emily Walter, University of Missouri-Columbia**  
**Anderson Lab (PSU), Shenoy Lab (Penn)**



Towards a Multiscale Computational Model of the Human Complement System for Predicting Immune Response in COVID-19 Patients

2:24 PM

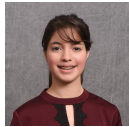
**Samantha Hall, Bryn Mawr College**  
**Radhakrishnan Lab (Penn)**



Nonbiased Transcriptomic Analysis Reveals that YAP and TAZ co-Transcriptional Activators Regulate Survival

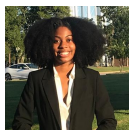
**2:36 PM**

**Serin Varughese, Drexel University  
Boerckel Lab (Penn)**

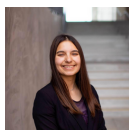


Quantifying repair factors in lipid loaded hepatocytes through image analysis

**2:48 PM**



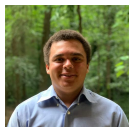
**Nadja Maldonado Luna, UPR Mayagüez  
Mariah Turner, Alabama State University  
Wells Lab (Penn)**



Strain Mapping to Identify the Mechanisms by which Ultrasound Activates Ion Channels

**3:00 PM**

**Sorina Munteanu, UC Merced  
Genin Lab (WashU)**



Assessing Nucleus Pulposus Phenotype Expression and Extracellular Matrix (ECM) Interaction via Mimetic Peptides in relation to Intervertebral Disc (IVD) Degeneration

**3:12 PM**

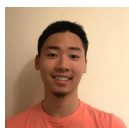
**Evan Morris, Washington University in St. Louis  
Huebsch Lab (WashU)**



The Role of the Microtubule Cytoskeleton in Helical Growth in Plant Roots

**3:24 PM**

**Lily Murchison, Scripps College  
Dixit Lab (WashU)**



Modeling fibroblast-led collective invasion of carcinoma cells with differing mechanically mediated factors

**3:36 PM**



**David Reynolds, Iowa State University  
Sabrina Shafi, City College of New York  
Pathak Lab (WashU)**



Scaling Relationships and Patient Survival in Fibrosis-Associated Gene Analysis

**3:48 PM**



**Kathryn Driscoll, Rowan University  
Harold Treminio, Johns Hopkins University  
Discher Lab (Penn)**

# UNDERGRADUATE RESEARCH SYMPOSIUM

July • 24 • 2020 | 1:30 - 4:00 PM EST

Zoom: <https://zoom.us/j/93191593690> | Password: 358615

Welcome Address

1:30 PM EST

Rebecca Wells and Ram Dixit, Directors of Education



Image Analysis to Examine Spatial Properties of the Pericellular Matrix within 3D Hydrogels

1:35 PM

**Bruce Enzmann, Johns Hopkins University**  
**Burdick Lab (Penn)**

Biomaterials, such as hydrogels, can be engineered with biophysical cues that enable the study of three-dimensional microenvironments that simulate aspects of native extracellular matrix and modulate cellular functions such as differentiation and matrix deposition. Recent data showed that the accumulation of deposited matrix in the pericellular region influences the interactions between cells and their engineered hydrogel environment; however, little is known about the spatial localization and density of newly secreted (nascent) matrix at the cell-hydrogel interface. Using a metabolic labeling technique, we fluorescently labeled nascent proteins deposited by bovine chondrocytes within 7 days upon encapsulation in covalently crosslinked 5 kPa and 20 kPa hyaluronic acid hydrogels. To examine spatial properties of these nascent proteins, we used ImageJ to generate nascent protein intensity profiles and developed new analysis tools to quantify nascent protein area and average intensity. Our results show significant increases in nascent protein area and intensity around chondrocytes embedded within 5 kPa hydrogels compared to 20 kPa hydrogels. These findings suggest that secreted matrix within 5 kPa hydrogels distributes further into the hydrogel, whereas the more densely crosslinked 20 kPa hydrogels restrict nascent matrix distribution. Moreover, lower nascent protein average intensity and area within 20 kPa hydrogels indicate that densely crosslinked hydrogels reduce nascent protein deposition. Ongoing work is analyzing the effect of culture time and local mechanical properties on nascent matrix deposition and distribution. We anticipate that these results have implications on hydrogel design for applications in tissue engineering and regenerative medicine.



Patterning Surfaces for Inducing Cardiomyocyte Alignment

1:47 PM

**Joenid Colón-Mateo, UPR-Cayey**  
**Andrea Plaza-Castro, UPR-Cayey**



**Christian Tessman, Johns Hopkins University**  
**Guvendiren Lab (NJIT)**



Wrinkles are a property found in many biological tissues. Scientists have tried to mimic these surface patterns to understand how cells mechanically interact with their microenvironment. Controlled surface patterns on gels have been shown to affect cell alignment, morphology, gene regulation, and differentiation. Here, wrinkle patterns were fabricated on polydimethylsiloxane (PDMS) substrates to regulate human cardiomyocyte (hCM) alignment, which is important for proper tissue function. PDMS sheets were subject to ultraviolet and ozone (UVO) treatment, with an initial strain of 20%, to form a thin film surface with a higher Young's modulus than the bulk. Exposure time was modified to determine its effect on wrinkle wavelength, amplitude and film thickness. Analysis of microscope images of the PDMS sheets showed that wrinkle wavelength and amplitude increased linearly with UVO exposure time, and that critical strain decreased linearly with time. The effect of wrinkling on hCM nuclei alignment was also investigated by culturing hCMs on flat and patterned PDMS sheets. Analysis of microscope images of the hCMs showed the average direction of nuclei alignment was similar for both topographical conditions:  $84.7 \pm 48.0$  degrees for flat and  $88.1 \pm 13.3$  degrees for patterned on day 4. However, the standard deviation of nuclei alignment on flat substrates was approximately three times greater than for patterned substrates. This indicates more uniform cellular nuclei alignment on patterned substrates. Development of materials that can mimic surface topography of tissues promises a greater understanding of the morphological response of cells leading to more diverse biomedical applications.



## Viscoelastic Properties of Tofu as a Phantom for Liver Disease Diagnosis

2:00 PM

**Katherine Kerr, Purdue University**  
**Janmey Lab (Penn)**

Liver disease is the cause of approximately two million deaths globally each year. Many liver diseases, such as liver fibrosis, are characterized by alterations in the mechanical properties of liver tissues. Magnetic resonance elastography (MRE) provides a noninvasive tool to diagnose and monitor liver disease by measuring the mechanical properties of tissues. To ensure accurate evaluations of tissue properties, materials called phantoms are often used to calibrate an MRE device. Traditional phantoms, such as polymeric gels, can be expensive, difficult to produce at large scales, and lack complex structures associated with liver tissue. Tofu offers a phantom candidate that is cheaper and easy to manufacture. In this work, the rheological properties of two types of commercial tofu, varying in firmness, were studied at different compression levels, making use of a home-made torsion pendulum. The pendulum was comprised of two aluminum plates, a labjack to which the tofu was fixed, and a rotary motion sensor. A cylindrical tofu sample was sandwiched between the labjack and plates. The plates were rotated by a small angle and then released. The subsequent oscillation angle was measured and used to infer the viscoelastic properties of tofu at various compression levels up to fifty percent. It was found that both types of tofu exhibited compression stiffening and shear softening properties, being qualitatively similar to liver properties. Our results suggest that tofu could be used as a tissue mimicking phantom to calibrate and validate MRE results.



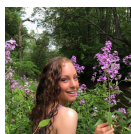
## Measuring and Modeling How Turgor Pressure-Driven Mechanical Forces Between Guard and Pavement Cells Underlie Stomatal Opening and Closing

2:12 PM

**Mythili Subbanna, Amherst College**  
**Emily Walter, University of Missouri-Columbia**  
**Anderson Lab (PSU), Shenoy Lab (Penn)**



Stomata are pores in the plant surface that facilitate photosynthesis and transpiration. In *Arabidopsis thaliana*, stomatal complexes comprise two kidney-shaped guard cells, and are flanked by neighboring pavement cells. The pathways by which cytosolic pressure changes, brought about by ion flux, drive cell inflation and deflation during stomatal opening and closing have been widely studied. However, the dynamic mechanical interactions between guard and pavement cells remain poorly understood. Here, we sought to identify how changes in guard cell shape might influence surrounding pavement cells. We hypothesized that during stomatal opening, guard cell area would increase, imposing stress on neighboring pavement cells, thus decreasing neighboring pavement cell size, with opposite trends for both during stomatal closure. We incubated seedlings in either fusicoccin plus light or abscisic acid (ABA) plus darkness to induce stomatal opening or closure, respectively, and measured changes in cell area over 2.5 hours. Fusicoccin-treated guard and non-neighboring pavement cells expanded relative to neighboring pavement cells. Conversely, ABA-treated guard cells shrank while ABA-treated neighboring pavement cells expanded. We developed a theoretical model to simulate stimulus-dependent changes in ion flux, osmotic potential, and guard and pavement cell size. Loading induced by guard cell expansion was predicted to cause pavement cell shrinking via an increase in hydrostatic pressure that drives fluid and ionic efflux. Realistic cell models were constructed using finite element software. Simulations were consistent with our hypothesis that stomatal opening imposes stress on neighboring pavement cells. These results provide new insights into plant mechanotransduction and turgor pressure regulation.



## Towards a Multiscale Computational Model of the Human Complement System for Predicting Immune Response in COVID-19 Patients

2:24 PM

**Samantha Hall, Bryn Mawr College**  
**Radhakrishnan Lab (Penn)**

Virion envelope flexibility and receptor spatial arrangement impacts immune modulation, recruitment, and internalization. Given the pandemic's topical nature, it is advantageous to investigate the mechanics of virion elicited immune response, and how it manifests in patients under pulmonary duress. The majority of COVID-19 deaths occur in patients who have Acute Respiratory Distress Syndrome (ARDS), an acute, diffuse, inflammatory lung injury caused by a variety of insults, most commonly pneumonia, sepsis, trauma, and COVID-19. ARDS affects 200,000 patients each year in the US, has a 40% mortality rate, and occurs in 25% of hospitalized COVID-19-infected patients, yet there are currently no FDA-approved drugs for ARDS. Inflammatory conditions resulting from ARDS are caused by the interaction between the virus and immune cells, namely neutrophils and macrophages. These signaling interactions are primarily mediated via the complement pathway, a part of the immune system that enhances the ability of antibodies to clear pathogens, playing a role in inflammation, host defense, and signaling adaptive immunity. In this project, using methods of systems biology, we look towards signaling models of the complement system to compartmentally understand this complex system. COPASI is a computer software that creates and solves mathematical models, encoding differential equations of biological processes, and was a part of the methodology behind this research. A previously existing computational model involving the enhancement and suppression mechanisms that regulate complement activity provided a template model in Systems Biology Markup Language (SBML) format, a standard form of systems biology XML codes (Liu et al, 2011). Plots were produced of complement regulation with inhibitors under infection inflammation conditions in terms of mediator protein deposition, and of positive feedback amplification of neutrophil activation. Results focused on three aspects: validation of existing data, exploring the amplification modules of the complement pathway, and characterizing emergent properties such as bistable switches regulating the complement cascade. The broader question to be explored in next steps involves how this modeled mechanism would work on the viral surface. Because the complement cascade occurs on the surface of the virus during neutrophil interaction, we believe that the mechanics of the virus, whether it is crystalline or noncrystalline (COVID-19 is noncrystalline), in conjunction with the spatial arrangement of the cascade proteins determine this behavior. Future work involving spatial and stochastic models will involve looking at mechanical and spatio-temporal criterion in virion interaction.



## Nonbiased Transcriptomic Analysis Reveals that YAP and TAZ co-Transcriptional Activators Regulate Survival

2:36 PM

**Serin Varughese, Drexel University**  
**Boerckel Lab (Penn)**

Yes-associated protein (YAP) and transcriptional co-activator with PDZ-binding motif (TAZ) are two mechanically activated transcriptional regulators that have been found to play a significant role in osteoprogenitor proliferation and differentiation during embryonic bone development and fracture healing. However, the specific gene interactions and pathways by which YAP and TAZ activate or repress these processes remains unclear. Therefore, the goal of this project was to analyze the differential expression of genes in YAP/TAZ depleted cells, and to use a non-biased gene ontology approach to identify which cellular processes these genes were involved with. In order to study gene expression changes in the absence of YAP and TAZ, we analyzed an existing data set generated in our laboratory in which bulk RNA expression profiles were measured in endothelial colony forming cells (ECFCs) transfected with siRNA to deplete YAP and TAZ. A differential gene expression analysis using this bulk RNA sequencing data identified 2,241 downregulated genes and 2,508 upregulated genes in YAP/TAZ siRNA samples. The gene expression profile of the YAP/TAZ siRNA samples reveals a relatively equal distribution of up and downregulated genes, suggesting that YAP and TAZ may interact directly or indirectly with signaling pathways to either promote or suppress certain biological processes in the cell. To investigate these findings further, a gene ontology (GO) analysis was conducted in order to classify these up or downregulated genes into clusters based on the cellular processes they are involved in. The results of this analysis showed that YAP/TAZ knockdown significantly reduced expression of several processes associated with cell cycle and functional protein synthesis, both of which play an integral role in cell proliferation and differentiation, respectively. A GO term analysis of genes that were upregulated in samples with YAP/TAZ knocked down revealed an enrichment of genes associated with the positive regulation of apoptotic processes. Taken together, these results indicate that when YAP/TAZ is absent, cells are not only experiencing decreased proliferation, but they are also actively undergoing cell death, suggesting that YAP and TAZ play a significant role in regulating the survival of the cell. By classifying differentially expressed genes based on their involvement in specific biological processes, these gene ontology results have provided us with a streamlined set of candidates YAP/TAZ associated genes that can be investigated in future experiments to determine the specific mechanisms that underly proliferation and apoptosis.



**Nadja Maldonado Luna, UPR Mayagüez****Mariah Turner, Alabama State University****Wells Lab (Penn)**

**Introduction:** Hepatocellular carcinoma (HCC) is the most common type of primary liver cancer, often occurs in people with chronic liver diseases, and the presence of cirrhosis is seen as the most significant risk factor [1]. Cirrhosis is characterized by alterations in the extracellular matrix (ECM), including increased deposition of collagen and alignment of the ECM architecture, which drastically increases tissue stiffness [2]. Although HCC is often associated with cirrhosis, it can also arise in non-cirrhotic livers in the context of non-alcoholic fatty liver disease (NAFLD) [3]. Lipid accumulation in the liver cells, characteristic in NAFLD, fills the cell cytoplasm and compresses the nucleus. Based on this morphology, the Wells Lab has hypothesized that the lipid droplets act as a mechanical stress on the nucleus, functioning similarly to tissue stiffness [4]. Nuclear deformation from external sources of mechanical stress, such as migration through constricted environments or culture on stiff substrates, has been shown to increase the frequency of nuclear rupture, leading to depletion of nuclear repair factors and the accumulation of DNA damage [5]. We suggest that deformation due to lipid droplets may similarly lead to the depletion of important repair factors and increased accumulation of double-stranded DNA breaks, which may increase the risk of HCC development in NAFLD livers. The objective of this study was to quantify the impact of lipid accumulation in liver cells (hepatocytes) on the amount of DNA damage repair factor in the cells.

**Materials and Methods:** **Cell culture:** Primary human hepatocytes (PHH) were seeded onto collagen-coated polyacrylamide (PAA) gels with storage modulus values of 500 and 10 kPa that are representative of the stiffness of normal and cirrhotic livers, respectively. Cells were also cultured on glass, which is non-physiologically stiff. **Fatty acid treatment:** After the seeding period, PHH cells were incubated for 48 h in the presence of 400 $\mu$ M oleic acid and 0.5% bovine serum albumin (BSA) solution in DMEM. Oleate is the second most common fatty acid in the human diet and is easily packaged into lipid droplets. **Cell staining, microscopy, and image analysis:** To identify the lipids and assess gross nuclei morphology, cells were stained with BODIPY and DAPI, respectively. To look at the amount of repair factor, BSA control and oleate-treated cells were stained for Ku80. Cells were imaged using a confocal microscope. Nuclei morphology (area, circularity, and solidity) was analyzed using semi-automated image segmentation and detection of individual nuclei in ImageJ. Ku80 mean intensity and integrated density of the nucleus was measured. One-way ANOVAs were used to test the statistical significance of lipid accumulation on nuclear deformation and on Ku80 staining intensity.

**Results and Discussion:** Nuclear area, circularity, and solidity for oleate-loaded cells tended to decrease compared to controls, consistent with previous work [4]. Also, Ku80 repair factor means intensity and integrated density decreased with lipid loading of cells seeded on the stiffest substrates. Ku80 mean intensity was associated with the nuclear area, however no strong association was seen for any of the measured shape parameters.

**Conclusions:** The results of these experiments were consistent with previous work from the lab, showing increased nuclear deformation and compression, and decreased repair factor intensity in oleate-treated cells. Ku80 mean intensity was also correlated with nuclear area, suggesting that nuclear compression may be a contributor to Ku80 decrease in oleate-treated cells. Furthermore, differences between the groups were highest on the stiffest substrates, indicating that some level of tissue stiffening may be required for lipid droplets to act as a mechanical stress. Future work aims to determine if lipid- droplet accumulation increases DNA damage accumulation, through a number of different potential mechanisms.

**References:** [1] Masuzaki+2009 J Hep. [2] Asselah+2009 Gut. [3] Kanwal+2018 Gastroenterology. [4] Chin+2020 AJP-Gastrointest Liver Physiol. [5] Ivanovska+2019 Biophysical Journal.



## Strain Mapping to Identify the Mechanisms by which Ultrasound Activates Ion Channels

3:00 PM

**Sorina Munteanu, UC Merced**  
**Genin Lab (WashU)**

Ultrasound imaging can be used as a therapeutic tool for neurological disorders through stimulation of certain mechanosensitive ion channels. However, the molecular mechanism through which these ion channels are activated is unknown. We hypothesize that ultrasound can cause a mechanical force that deforms the cells, thus activating ion channels. To test this hypothesis, *Xenopus* oocyte membranes will be analyzed in vitro by confocal microscopy to further elucidate the deformation caused by ultrasound. To evaluate whether ion channel activation relates to mechanical strain, these experiments require real-time estimations of strain fields over the oocyte membrane. We therefore developed a method by which stacks of confocal images could be computationally and quantitatively observed to reveal mechanical changes. Through strain mapping under two- and three-dimensional conditions, the deformation is quantified through displacement tracking. With three-dimensional renderings of the oocytes under strain, normal vectors reveal the expansion or shrinkage of the membrane in the xy plane. Thus, the strain fields could be estimated for subsequent correlation with the activation of mechanosensitive ion channels. We show that the controlled membrane expands laterally and retracts longitudinally as tension is applied at magnitudes that are reasonable estimates of those expected from loading by ultrasound. Elucidating the mechanisms of ultrasound on mechanosensitive ion channels may provide the field of neuroscience with a powerful tool that is comparable to techniques such as optogenetics. The underlying mechanisms of ultrasound could be applied clinically as a therapeutic modality for diseases such as Parkinson's, depression, and anxiety.



## Assessing Nucleus Pulposus Phenotype Expression and Extracellular Matrix (ECM) Interaction via Mimetic Peptides in relation to Intervertebral Disc (IVD) Degeneration

3:12 PM

**Evan Morris, Washington University in St. Louis**  
**Huebsch Lab (WashU)**

{Abstract retracted}

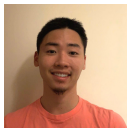


## The Role of the Microtubule Cytoskeleton in Helical Growth in Plant Roots

**Lily Murchison, Scripps College**  
**Dixit Lab (WashU)**

3:24 PM

Roots are critical organs for finding needed nutrients for plants and using directional growth to avoid foreign obstacles. Plant roots, which are anatomically symmetrical, grow via turgor pressure-driven cell expansion. Plant cells are encompassed by cortical microtubules that guide the deposition of cell wall materials which reinforces the cell wall along the transverse axis in elongating cells and direct cell growth in the vertical direction. Mutations in proteins that interact with microtubules can cause helical growth. The *spr1-3* mutant is a point mutation that tracks the growing plus-end of microtubules and produce a right-handed growth pattern. A skewed orientation of the microtubule array has been implicated in causing twisted plant growth in mutants, however the role of skewed microtubules in promoting twisted root growth is not well understood. Furthermore, it is unclear if twisting also occurs at the cell level. Using *Arabidopsis thaliana*, a commonly used plant for cytoskeletal research, we compared the *spr1-3* mutant to wild-type Col-0 to better understand the role microtubule orientation has within this twisted phenotype and what relationship the microtubules have with the morphology of the cells, ultimately aiming to understand how patterns at the cytoskeletal and cell level contribute to this twisted phenotype. To assess if microtubules are skewed prior to the onset of root twisting, microtubule orientation in Col-0 and *spr1-3* roots expressing a GFP-TUB6 marker were measured using the FibrilTool ImageJ tool. We found that microtubules in *spr1-3* roots adopt a left-handed skew before twisting occurs, suggesting that skewed microtubule array may be what drives the twisting phenotype to occur at the organ level. To assess twisting at the cell level, morphometry of wall lengths and angles were compared between wild-type Col-0 and *spr1-3* roots using ImageJ. From this we found that at the cell level symmetry breaks in lateral wall lengths whilst maintaining its symmetry in cell angles. This study will help further inform us how microtubule-level mutations affect cell-level and organ-level directional growth and can be used for future modeling of root skewing.



Modeling fibroblast-led collective invasion of carcinoma cells with differing mechanically mediated factors

3:36 PM

**David Reynolds, Iowa State University**



**Sabrina Shafi, City College of New York**

**Pathak Lab (WashU)**

Prevention of cancer cell dissemination and secondary tumor formation is a major goal of cancer therapy as a majority of cancer deaths are related to metastasis. Metastasis is initiated by the collective invasion of carcinoma cells into local epithelial tissue. Carcinoma cells are able to migrate away from the initial site by following the mechanically-mediated signalings produced by the stromal fibroblasts. Computational modeling offers a simplistic way of isolating the key factors responsible for cancer cell invasion, which is not a possibility in vivo and in vitro studies. By utilizing CompuCell3D software, our model reveals that force-applied fibroblasts with low adhesion energies between fibroblasts and cancer cells demonstrate characteristics of cancer cell invasion as described in the literature. In the future, protease-mediated pathways can also be integrated into the model to better represent the biological phenomena. Using computational models to reproduce cancer cell migration can identify key modulators of its early metastasis.



Scaling Relationships and Patient Survival in Fibrosis-Associated Gene Analysis

3:48 PM

**Kathryn Driscoll, Rowan University**



**Harold Treminio, Johns Hopkins University**

**Discher Lab (Penn)**

KD: Bulk mRNA-seq data obtained from The Cancer Genome Atlas (TCGA) can be used to elucidate gene expression and gene scaling relationships across cancers in order to identify common genes and groups of genes that predict significant survival changes in a cohort of patients. In this analysis, gene scaling relationships among two fibrosis-associated genes of interest (COL1A1 and ACTA2) and four urinary tract cancers were assessed for survival trends across data sets. Bladder cancer (BLCA), Kidney Chromophobe Cancer (KICH), Kidney Clear Cell Carcinoma (KIRC), and Kidney Papillary Cell Carcinoma (KIRP) were chosen for this analysis because they represent a common system and each cancer expressed gene scaling for each gene of interest. For COL1A1, a gene associated with fibrosis and positive survival trends in other cancers, KIRC and KIRP showed significantly decreased survival of high expressors of the gene and none of the cohorts showed improved survival. Further, in ACTA2, a gene associated with cancer metastasis and fibrosis, only KIRP and BLCA showed significantly reduced survival with KICH indicating non-significant positive survival with high ACTA2 expression. A significant finding in this analysis is that COL5A1, COL6A3, and COL1A2 not only scaled with COL1A1 in all four cancers, but also predicted significantly poor survival with elevated expression in two of the four urinary cancers. These genes are associated with tumor growth and poor prognosis in both urinary cancers and cancers from other systems. Furthermore, PLN and CNN1 scaled with ACTA2 across all four cancers and indicated negative survival in two of the four. CNN1 has been identified as a possible oncogene in bladder cancer related to poor survival outcomes and PLN has not been previously explored in the context of cancer prognosis<sup>6</sup>. Taken together, these genes have potential as targets for gene therapies and as prognostic biomarkers. Since many of these genes indicate fibrosis, emerging ultrasound technology could be used as a non-invasive detection tool for urinary cancers.

HT: Cancer is responsible for one of the biggest counts of death in the world and continues to be studied for understanding survival and cures. Many components go into the growth and survival of tumors, but they all share common characteristics such as tissue stiffness. The regulation of specific genes in tissues often involve physicochemical processes which cause tissues to become stiff. Within the extracellular matrix (ECM), gene-gene power laws can be used to determine gene scaling with tumors found in The Cancer Genome Atlas (TCGA) and their respective RNA-seq data. Out of the thirty-two possible cancer options, four were studied because of their relationship in mostly affecting females: ovarian (OV), cervical (CESC), uterine (UCS), and breast (BRCA) cancer. The two genes that were studied were COL1A1 and ACTA2, two genes which positively correlate with tumor metastasis and fibrosis. From generated survival plots, it was observed that COL1A1 is highly involved in ECM organization, while ACTA2 is involved in angiogenesis and cell migration with respect to their strong scaling genes. Many of the trends showed no significant predictions of survival within the scaling genes. However, data suggested that strong scaling genes with ACTA2 in Ovarian and Cervical cancers were also significantly involved in ECM organization. When further compared, the genes that scaled strongly with ACTA2 and COL1A1 had significant overlap, which was not observed within the other gynecological cancers. Although breast and uterine cancers do not spark any outstanding data, ovarian and cervical cancers suggest that there are other processes occurring in these tumors which are not normally occurring in other tissues.